*The Korean Journal of Ceramice*, **5**[3] 288-295 (1999)

# Electrical Conduction in $SrZr_{0.95}Y_{0.05}O_{2.975}$ Ceramics

**Hyun-Deok Baek and Jin-Hyo Noh**

*Department of Materials Science and Engineering, Hong-ik University, Chochiwon, Chungnam 339-800, Korea*

(Received September 23, 1998)

Partial conductivities contributed by electron holes, oxygen ions, and protons were calculated in $SrZr_{0.95}Y_{0.05}O_{2.975}$, using the reported formulae derived from the defect chemistry of HTPCs Required parameters were obtained from the graphical analysis of total conductivity variation against partial pressure of water vapor and oxygen. Predicted overall conductivities showed a reasonable agreement with experimental measurements. The conductivity of the material showed a linear increase with square root of the water vapor pressure. This increase was due to proton conduction and an indication of a low proton concentration. The calculation of partial conductivities at 800°C resulted in an almost pure ionic conductivity at $P_{O2}=10^{-10}$ atm and a predominant hole conductivity at $P_{O2}=0.20$ atm. Pure proton conduction was not expected at this temperature, contrary to the earlier reports. Discussions were made in relation with reported thermodynamic data and defect structure of the material. It was shown that from the total conductivity dependence on water vapor pressure, the pure ionic conductivity at low oxygen partial pressures could be separated into protonic and oxygen ionic conductivity in $ZrO_2$-based HTPCs.

***Key words:*** $SrZr_{0.95}Y_{0.05}O_{2.975}$, HTPCs, Graphical analysis, Partial conductivities, Proton concentration

## I. Introduction

Many oxides are mixed conductors, in which electrical charges are carried by electrons and oxygen ions. Some perovskite-type oxides such as $BaCeO_3$ and $SrZrO_3$ when doped with rare-earth oxides, exhibit proton conduction in the hydrogen-containing atmosphere. The oxides dissolve water vapor (or hydrogen) from atmosphere through oxygen ion vacancies and produce protonic defects.[1,2] The concentrations of charge- carrying defects are functions of both oxygen and water content in the ambient gas, and thus the investigation of the electrical conductivities are rather complex. In this circumstance, modeling was considered as an appropriate technique in the prediction of electrical conductivities at various gaseous atmosphere.[3-5] For the calculation of partial conductivities by each defect, required kinetic and thermodynamic parameters were determined from just total conductivity measurements and a graphical analysis based on the defect structure known for high-temperature proton-conductors (HTPCs). The details of the modeling could be referred to our earlier publications,[4,5] but were repeated here for the sake of the readability of the present paper.

The relevant equilibria describing the effects of gas phase on the defect chemistry of $ABO_3$-based proton conducting materials have been well established and can be summarized by the following two equations.

$$V_o + 1/2O_2(g) \rightleftarrows O_o + 2\dot{h} \quad (1)$$

$$H_2O(g) + V_o + Oo \rightleftarrows OH_o \quad (2)$$

Eligible defects considered were electron holes, protons, and oxygen vacancies in oxygen atmosphere. Applying mass action law for the defect equations and appropriate electro-neutrality condition, partial conductivities contributed by these defects were derived as functions of partial pressure of water vapor and oxygen.[5,6] Assuming mobility of the defect is independent of its concentration, the partial conductivities by the defects were expressed in the following equations.

$$\sigma_H/\sigma_H^* = \{[1+\alpha/P_w]^{1/2}-1\}P_w/[(1+\alpha)^{1/2}-1] \quad (4)$$

$$\sigma_v/\sigma_v^* = [[1+\alpha/P_w]^{1/2}-1\}^2 P_w/\alpha \quad (5)$$

$$\sigma_h/\sigma_h^* = \{[1+\alpha/P_w]^{1/2}-1\} (P_w/\alpha)^{1/2}P_{O2}^{1/4} \quad (6)$$

$\sigma_H$, $\sigma_V$, and $\sigma_h$ denote partial conductivities by protons, oxygen ions, and electron holes, respectively. $P_w$ is water vapor pressure in atmosphere. $\sigma_H^*$ is protonic conductivity at $P_w$=1 atm and $\sigma_h^*$ is hole conductivity at $P_{O2}$=1 atm and $P_w$=0 atm. $\sigma_v^*$ is oxygen ion conductivity at $P_w$=0 atm. Parameter=$8y/K_2$. y is the concentration of acceptor dopant $[M_{Zr}']$. M is usually a rare earth element substituting for B-site in $ABO_3$-based perovskites. $K_2$ is the equilibrium constant for the hydration reaction, Eq. (2). Employing a new variable R, and functions f(R) and g(α) by setting $R=P_w/\alpha$, $f(R)=(1+R)^{1/2}-R^{1/2}$, and $g(\alpha)=\alpha/[(1+\alpha)^{1/2}-1]$, the partial conductivities can be given as follows.

$$\sigma_H=\sigma_H^* f(R)R^{1/2}g(\alpha) \quad (7)$$

$$\sigma_v=\sigma_v^* f^2(R) \quad (8)$$

$$\sigma_h=\sigma_h^* f(R)P_{O2}^{1/4} \quad (9)$$

Only $\sigma_h$ is a function of $P_{O2}$, and thus if $\sigma_{tot}$ is plotted against $P_{O2}^{1/4}$, one obtains the intercept(a) and the slope(b) as;

$$a=\sigma_H+\sigma_v,\ b=\sigma_h^* f(R) \quad (10)$$

Eq. (10) allows to separate ionic conductivity($\sigma_H+\sigma_V$) from total conductivity. This is indirect, but taken as a reliable technique for the determination of ionic transference number.[7,8] For the cases $R \ll 1$, $(1+R)^{1/2} \approx 1+(1/2)R-(1/8)R^2$, and thus $f(R) \approx 1-R^{1/2}+(1/2)R-(1/8)R^2$. Then total conductivity can be expressed as Eq. (11)

$$\begin{aligned}\sigma_{tot}&=\sigma_v+\sigma_h+\sigma_H\\ &=p+qR^{1/2}+rR+sR^{3/2}+tR^2+\cdots\end{aligned} \quad (11)$$

where $p=\sigma_v^*+\sigma_h^*P_{O2}^{1/4}$, $q=\sigma_H^*g(\alpha)-2\sigma_v^*-\sigma_h^*P_{O2}^{1/4}$, $r=-\sigma_H^*g(\alpha)+2\sigma_v^*+\sigma_h^*P_{O2}^{1/4}$, $s=(1/2)\sigma_H^*g(\alpha)-\sigma_v^*$, $t=-(1/8)\sigma_h^*P_{O2}^{1/4}$

If $R \ll 1$, then $R^{1/2} \gg R \gg R^{3/2} \gg \cdots$, and overall conductivity can be approximated as $\sigma_{tot} \approx p+qR^{1/2}$. The total conductivity variation is, therefore, expected to be linear in $_{tot}$ vs. $P_w^{1/2}$ plot. The intercept (a') and slope (b') of $\sigma_{tot}$ vs. $P_w^{1/2}$ plot can be given as,

$$a'=\sigma_v^*+\sigma_h^*P_{O2}^{1/4},\ b'=\sigma_H^*g(\alpha)-2\sigma_v^*-\sigma_h^*P_{O2}^{1/4}/\alpha^{1/2} \quad (12)$$

Experimental determination of a, a', b, and b' allows to obtain the parameters $\sigma_H^*$, $\sigma_v^*$, $\sigma_h^*$, and $\alpha$ for the calculation of partial conductivities.

## II. Experimental Procedure

### *1. Preparation of samples*

$SrZr_{0.95}Y_{0.05}O_{2.975}$ powder was synthesized via solid-state reaction as shown in Fig. 1. Starting powders, $SrCO_3$ (Shinyo), $ZrO_2$(Yakuri), and $Y_2O_3$(Aldrich) with the desired stoichiometric ratio, were ball-milled for 6 hours in acetone. The powder mixture was dried and calcined in air at 1000°C for 10 hours. The calcine was ground, mixed with a binder, PVB, and then dissolved in acetone. Then acetone was dried out and the powder was fabricated into cylindrical pellets with 1 cm diameter, using uniaxial die-press under a pressure of 294 MPa. The pellets were sintered in air at 1600°C for 12 hours. X-ray powder diffraction analysis of the final products, as shown in Fig. 2, identified a perovskite phase same as that reported in the literature.[9] The bulk density of the sintered pellets was measured with Poresizer 9320(Micrometrics) and found to be 93% of the theoretical value.

### *2. Measurements of electrical conductivity*

Electrode was prepared by applying Ag paste on both faces of pellets and baked in air. Impedance spectroscopy measurements was performed with 0.08V AC signal, using Solartron model 1255 Frequency Response Analyzer at 800°C. The frequency range applied was $1\sim2\times10^7$ Hz. The schematic of measuring apparatus was given in Fig. 3. Oxygen partial pressures were controlled by flowing pure oxygen, nitrogen, argon, air or mixture of these gases. Water vapor pressure was varied by changing the water bath temperature. The furnace temperature was checked by placing a K-type thermocouple near the specimen. Oxygen partial pressure was monitored in the exit gas by an zirconia oxygen sensor. The gas flow rate was maintained 250 cc/min. The partial pressure of water vapor and oxygen adopted in the experiment is shown in Table 1.

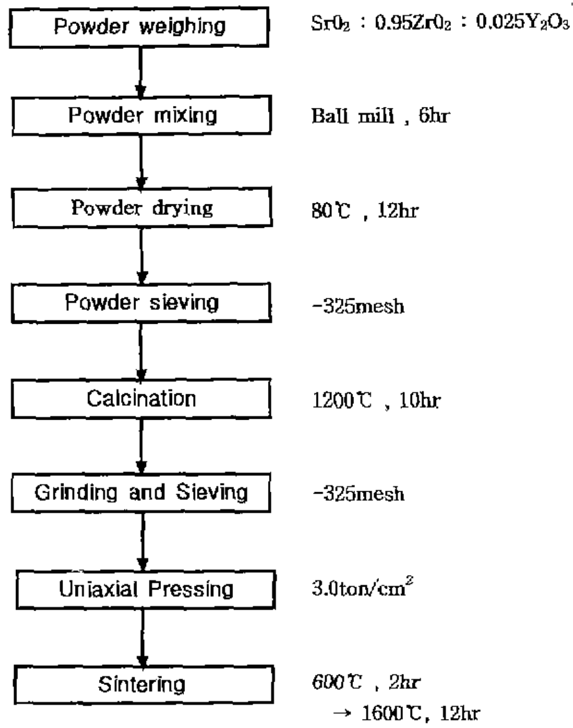


**Fig. 1.** Preparation of sintered pellets of $SrZr_{0.95}Y_{0.05}O_{2.975}$.

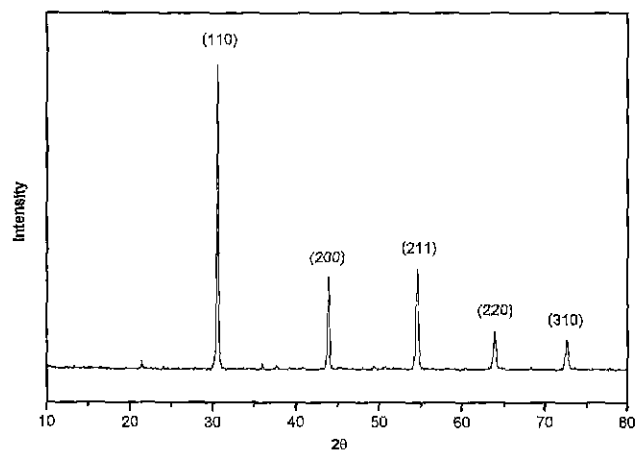


**Fig. 2.** XRD diffraction patterns of $SrZr_{0.95}Y_{0.05}O_{2.975}$.

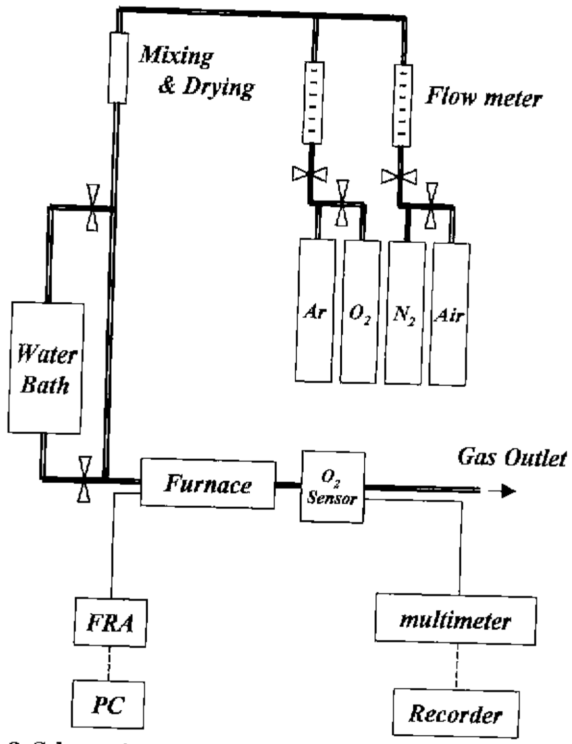


**Fig. 3.** Schematic of measuring apparatus.

## III. Results

Two semicircles were observed in the impedance plane as shown in Fig. 4. The high frequency one in the left-hand side was due to the bulk resistance of the specimen, while the other one was ascribable to the electrode polarization. This was confirmed by applying different electrode materials, Pt and Ag paste. At several $P_{O2}$'s given in Table 1, the conductivity increased with water vapor pressure. At $P_{O2}$ of $1.5\times110^{-5}$ atm, $\sigma_{tot}$ vs. $P_w^{1/2}$ plot was given in Fig. 5. The linear fit of total conductivity gives the intercept and the slope as follows.

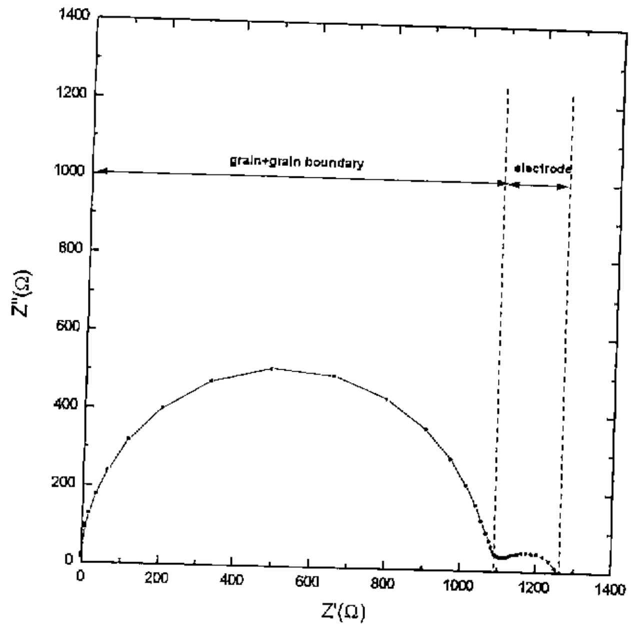


**Fig. 4.** Complex impedance diagram at $P_w$=12.55×$10^{-3}$ and $P_{O2}$= 1.42×$10^{-4}$ atm

$$\sigma_v^{*}+\sigma_h^{*}P_{O2}^{1/4}=1.72\times10^{-4} \tag{13}$$
$$[\sigma_h^{*}g(\alpha)-2\sigma_v^{*}-\sigma_h^{*}P_{O2}^{1/4}]/\alpha^{1/2}=10.72\times10^{-4} \tag{14}$$

On the other hand, $\sigma_{tot}$ vs. $P_{O2}^{1/4}$ plot at $P_w$=9.55×$10^{-3}$ atm is given in Fig. 6. The plot showed an excellent linearity and following equations were obtained.

$$\sigma_H+\sigma_v=2.33\times10^{-4}\mathrm{Scm^{-1}} \tag{15}$$

$$\sigma_h^{*}f(R)=6.99\times10^{-4}\mathrm{Scm^{-1}atm^{-1/4}} \tag{16}$$

**Table 1.** Partial Pressures of Water Vapor and Oxygen Adopted in the Conductivity Measurement

| Gas | Water bath t/°C | Pw/$10^{-3}$ atm | Measured voltage/mV | Average mV | $P_{O2}$/atm |
|---|---|---|---|---|---|
| $O_2$ | 3.5<br>5.6<br>10.5<br>14.5 | 7.75<br>9.55<br>12.55<br>16.30 | −35.44±4.90<br>−36.17±6.39<br>−36.63±5.11<br>−36.14±3.54 | −36.095 | 1.00 |
| Air | 3.5<br>6.5<br>10.5<br>14.5 | 7.75<br>9.55<br>12.55<br>16.30 | 1.005±1.602<br>0.999±1.322<br>0.997±1.601<br>0.951±1.468 | 0.988 | 0.201 |
| Ar+$O_2$ | 3.5<br>6.5<br>10.5<br>14.5 | 7.75<br>9.55<br>12.55<br>16.30 | 44.90±6.18<br>41.62±5.68<br>40.95±6.23<br>39.94±7.16 | 41.853 | 3.42×$10^{-2}$ |
| Ar | 3.5<br>6.5<br>10.5<br>16.30 | 7 75<br>9.55<br>12.55<br>16.30 | 167.93±7.72<br>167.27±7.00<br>168.84±12.53<br>169.69±9.42 | 168.432 | 1.42×$10^{-4}$ |
| $N_2$ | 3.5<br>6.5<br>10.5<br>14.5 | 7.75<br>9.55<br>12.55<br>16.30 | 222.63±14.84<br>218.45±14.26<br>221.54±15.04<br>217.52±13.28 | 220.035 | 1.51×$10^{-5}$ |

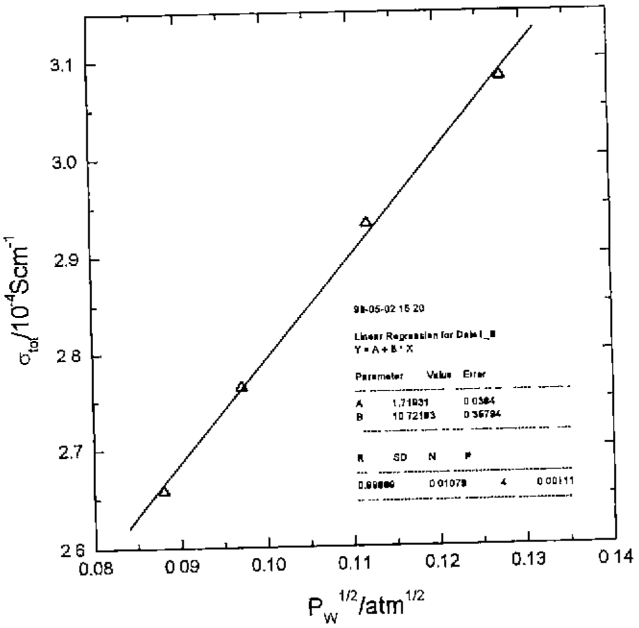


**Fig. 5.** $\sigma_{tot}$ vs. $P_w^{1/2}$ plot at $P_{O2}=1.51\times10^{-5}$ atm and 800°C.

**Table 3.** Determined Parameters

| Parameters | α | $\sigma_H^*/Scm^{-1}$ | $\sigma_v^*/Scm^{-1}$ | $\sigma_h^*/Scm^{-1}$ |
|---|---|---|---|---|
| | 10< | $10.2\times10^{-4}$ | $1.28\times10^{-4}$ | $7.03\times10^{-4}$ |

The values of the four parameters can be determined from Eq. (13) through (16). For an arbitrary value of α, $\sigma_h^*$ is calculated (Eq. 16), which is in turn used to obtain $\sigma_v^*$ and $v_H^*$ (Eq. 13 and 14). For different α values, the calculation was iterated until Eq. (15) was satisfied. In Table 2, the calculation results were given for increasing α 's. The variation of the parameters with α is so slow for $\alpha\geq10$ that giving a definite value of α was impossible, and the approximated parameters were listed in Table 3. Total conductivities were calculated with α value of 250 (the evaluation of α will be mentioned later) and compared with those measured at various oxygen partial pressures. This large α value justifies the linearity of the $\sigma_{tot}$ vs. $P_w^{1/2}$ plot in a rather wide range of water vapor pressure. As given in Fig. 7, the predicted conductivities showed good agreements with experimental measurements. When other α values larger than 10 were applied, similar results were

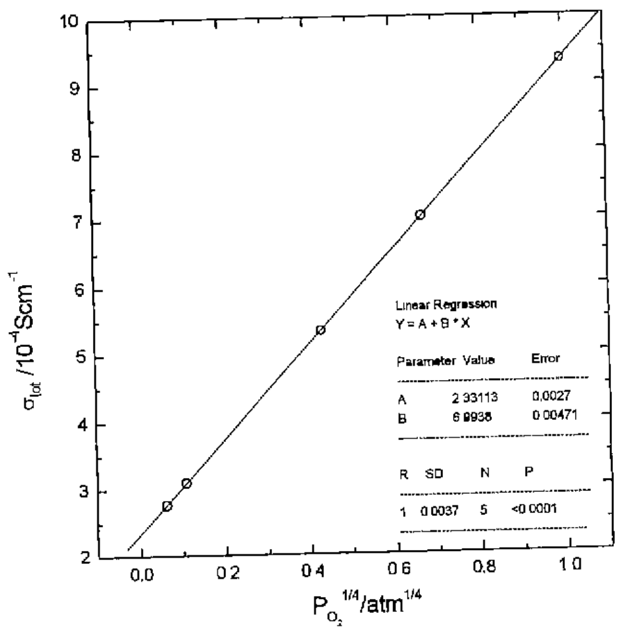


**Fig. 6.** $\sigma_{tot}$ vs. $P_{O2}^{1/4}$ plot at $P_w=9.55\times10^{-3}$ atm and 800°C.

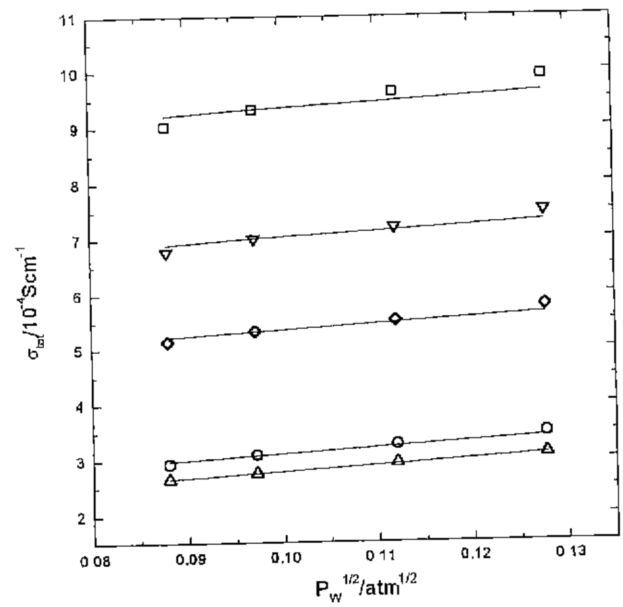


**Fig. 7.** Total conductivity against $P_w^{1/2}$ at 800°C. $P_{O2}$(atm); □ : 1.00($O_2$), ▽: 0.201(Air), ◇: 3.42*$10^{-3}$(Ar+$O_2$), ○: 1.42*$10^{-4}$ (Ar), △: 1.51*$10^{-5}$($N_2$).

**Table 2.** Parameters Calculated with Increasing Values

| α | f(R) | g(α) | $\sigma_h^*/10^{-4}$ $Scm^{-1}$ | $\sigma_v^*/10^{-4}$ $Scm^{-1}$ | $\sigma_H^*/10^{-4}$ $Scm^{-1}$ | $\sigma_H+\sigma_v/10^{-4}$ $Scm^{-1}$ |
|---|---|---|---|---|---|---|
| 1 | 0.9070 | 2.4142 | 7.711 | 1.2389 | 5.667 | 2.2319 |
| 10 | 0.9696 | 4.3166 | 7.213 | 1.2699 | 8.547 | 2.2993 |
| 100 | 0.9903 | 11.0499 | 7.062 | 1.2793 | 9.975 | 2.3212 |
| 250 | 0.9938 | 16.8430 | 7.037 | 1.2809 | 10.243 | 2.3249 |
| 500 | 0.9956 | 23.3830 | 7.024 | 1.2817 | 10.381 | 2.3268 |
| 1000 | 0.9969 | 32.6386 | 7.015 | 1.2823 | 10.480 | 2.3282 |
| 2000 | 0.9978 | 45.7325 | 7.009 | 1.2826 | 10.551 | 2.3291 |
| 3000 | 0.9982 | 55.7814 | 7.006 | 1.2828 | 10.582 | 2.3295 |

obtained. The tendency of poorer agreements was observed at high oxygen pressures. The $\sigma_{tot}$ vs. $P_w^{1/2}$ plots at various $P_{O2}$ are not presented here, but the slope in the plot became larger with increasing $P_{O2}$, contrary to the prediction by Eq. (12). This fact is likely to be related with the deviation of data at high oxygen partial pressures.

## IV. Discussion

Thermodynamic parameter $\alpha$ equals $8y/K_2$, and $K_2$ is equilibrium constant for the water dissolution reaction given by Eq. 2. $K_2$ values were reported as a function of temperature for various proton-conducting oxides,[10] and for Y-doped $SrZrO_3$, $K_2$ was read as 0.335 atm$^{-1}$ at 800°C. This $K_2$ value corresponds to $\alpha$ of 11.9, which is in the range of $\alpha$ determined in this work. $K_2$ of Y doped-$SrZrO_3$ was lower than other HTPCs such as Y doped-$SrCeO_3$, Ca doped-$GdErO_3$, and Ca doped-$Ba_3(Nb_2Ca)O_3$, suggesting lower equilibrium solubility of protons in the material. This low $K_2$, or large $\alpha$, was suggested from the increasing conductivity with $P_w^{1/2}$. A large and thus high g($\alpha$) in Eq. (12) gives a higher possibility of a positive slope in the $\sigma_{tot}$ vs. $P_w^{1/2}$ plot. This $\alpha$ value is compared with those of other perovskites reported in the literature: 0.18 in $SrCe_{0.95}Yb_{0.05}O_{2.975}$ at 950°C,[11] and 0.35 and 0.05, respectively for $BaTh_{0.9}Nd_{0.1}O_{2.95}$ at 990°C and $BaTh_{0.9}Y_{0.1}O_{2.95}$ at 1003°C,[5] and negative slopes were observed in the $\sigma_{tot}$ vs. $P_w^{1/2}$ plot in all these systems.[12-14] Besides a high $\alpha$, a large $\sigma_H^*$ can also lead to a positive slope, regardless of $\alpha$ value. $\sigma_H^*$ is larger than $\sigma_v^*$ or $\sigma_h^*$ for $SrZr_{0.95}Y_{0.05}O_{2.975}$ as shown in Table 3. These values are compared with those of the perovskites having negative slopes; $\sigma_h^*$ has much larger than $\sigma_H^*$ or $\sigma_v^*$. Thus it can be said that Y-doped $SrZrO_3$ meets both of the two conditions for the positive slope; a large $\alpha$ and comparatively higher $\sigma_H^*$ value than $\sigma_H^*$ or $\sigma_v^*$ of the material at the given temperature.

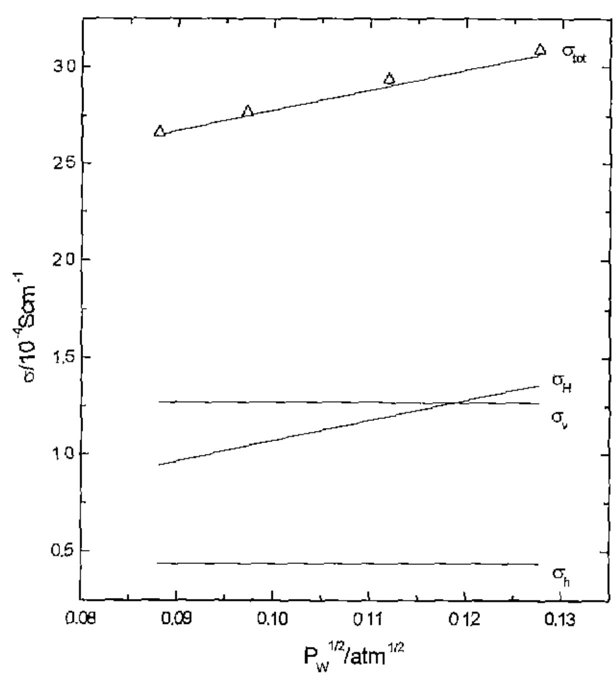


**Fig. 8.** $\sigma_{tot}$ vs. $P_w^{1/2}$ plot at $P_{O2}=1.51\times10^{-4}$ atm.

In Fig. 8 partial conductivities are given against $P_w^{1/2}$ at argon atmosphere ($P_{O2}=1.51\times10^{-5}$ atm). $\sigma_{tot}$ and $\sigma_H$ are linearly increasing, and $\sigma_v$ and $\sigma_h$ appears constant, independent of water vapor pressure. This is because, for large $\alpha$ values, f(R) is close to unity and partial conductivities given by Eq. (7) through (9) can be approximated as follows.

$$\sigma_H \approx \sigma_H^* P_w^{1/2} \tag{17}$$

$$\sigma_v \approx \sigma_v^* \tag{18}$$

$$\sigma_h \approx \sigma_h^* P_{O2}^{1/4} \tag{19}$$

The same expressions for the partial conductivities were obtained in the extreme cases, $[V_o^{\cdot\cdot}] \ll [OH_o^{\cdot}]$ for the general HTPCs.[6] The same formulae were also observed for In-doped $CaZrO_3$, of which proton concentration was considered very low and $[V_o^{\cdot\cdot}]$=constant.[15] Therefore, we can say that electro-neutrality of these electrolytes is maintained almost entirely by oxygen ion vacancies. In recent studies,[10,16] they found the proton solubility in relation with packing density of the structure. The hydration enthalpy, $\triangle H^o$ of Eq. (2) become less negative with increasing packing density in perovskite oxides. $ZrO_2$-based perovskites shows a high packing density as a result of small B-cation in the type $ABO_3$ and give a low value of $K_2$.

Besides the low equilibrium constant K, low proton concentration was explained by low activity coefficients of oxygen ion vacancy.[10,17] In general, defect equilibria may be affected by long or short range defect interaction or lattice relaxation.[18] The saturation limit of protons was observed in HTPCs, which is lower than expected value, i.e. $[OH_o^{\cdot}]<2[V_o^{\cdot\cdot}]=y$.[1,10,11] If activity coefficients are taken into consideration, the mass action law gives the respective equilibrium constant for Eq. (1) and (2) as follows.

$$K_1=(f_h p)^2/f_v[V_o^{\cdot\cdot}]P_{O2}^{1/2} \tag{20}$$

$$K_2=(f_H[OH_o^{\cdot}])^2/f_v[V_o^{\cdot\cdot}]P_w \tag{21}$$

where $f_h$, $f_H$ and $f_v$ denote activity coefficients of electron holes, protons and oxygen ion vacancies, respectively. Rewriting of Eq. (20) and (21) gives

$$p^2/[V_o^{\cdot\cdot}]P_{O2}^{1/2}=K_1 f_v/f_h^2 \tag{22}$$

$$[OH_o^{\cdot}]^2/[V_o^{\cdot\cdot}]P_{O2}^{1/2}=K_2 f_v/f_H^2 \tag{23}$$

Thus activity coefficients can be incorporated to relevant defect equilibria by substituting $K_1 f_v/f_h^2$ and $K_2 f_v/f_H^2$ for $K_1$ and $K_2$, respectively.

In $SrZr_{0.95}Y_{0.05}O_3$, saturated proton concentration is very low and most of the oxygen ion vacancies are sustained even under $P_w$=1 atm.[10,17] Accordingly we could assume that the activity coefficients for the two ionic defects are weak functions of the partial pressures of the corresponding gaseous species in the surroundings, and partial conductivities can be given by the same expressions as Eq. (4) through (6). Considering activity coefficients, $\alpha=8\ f_H^2 y/K_2 f_v$. Schober gave $f_H$ as a function $[OH_o]$, i.e. $f_H=1+m[OH_o]$ (with m=−0.6 for $BaIn_{0.5}Sn_{0.5}O_{2.75}$). However, in $SrZr_{0.95}Y_{0.05}O_3$, saturated concentration of proton is as low as $0.8\times10^{-3}$[17] and $f_H$ may be reasonably assumed as unity. $f_v$ is low for $ZrO_2$-based perovskites and $f_v$=0.03 from the reference.[10] Then α=239 with given values of $K_2$=0.0335 and y=0.03. Det-ailed discussion on y value will follow.

In addition to the equilibrium constant, the concentration of proton is influenced by other facts. One is the distribution of the dopant over the two cation sites, $M_{Zr}'$ and $M_{Sr}^{\cdot}$.[17,19] Another one we can consider is intrinsic schottky defects given by Eq. (24).[20]

$$nil=V_{Sr}''+V_{Zr}''''+3V_o \quad (24)$$

Taking these two facts into account, electro-neutrality condition requires to satisfy Eq. (25).

$$2[V_o^{\cdot\cdot}]+[OH_o^{\cdot}]=[M_{Zr}']-[M_{Sr}^{\cdot}]+2[V_{Sr}'']+4[V_{Zr}''''] \quad (25)$$

Now $y=[M_{Zr}']-[M_{Sr}^{\cdot}]+2[V_{Sr}'']+4[V_{Zr}'''']$. Müller[17] observed the composition $(Sr_{0.99}Y_{0.01})(Zr_{0.96}Y_{0.04})O_{2.975}$ for nominally 5% Y-doped $SrZrO_3$ single crystal, which corresponds to $[M_{Zr}']-[M_{Sr}^{\cdot}]=0.03$. Intrinsic schottky defects become insignificant in the acceptor-doped condition,[19] and thus the cation vacancies were considered negligibly small. As a result we obtained y=0.03. Here one could see the significance of the parameter α. It includes not only thermodynamic consideration of the defects but the effects from defect structure of the material.

In Fig. 9 partial and total conductivities versus water vapor pressure are given at two different oxygen partial pressures, $P_{O2}$=0.20 and $10^{-10}$ atm. As $\sigma_H$=0 in dry condition, the material is inherently mixed conductor by electron holes and oxygen ions. The relative contribution of electron holes is obvious at the two oxygen pressures. The material becomes almost pure ionic-conducting at $P_{O2}$ as low as of $10^{-10}$ atm. Oxygen ion conductivity are almost constant even with increasing water vapor pressure, suggesting that only small fraction of oxygen ion vacancies are filled by dissolution of water vapor. At $P_w$ of around 0.01 atm, $\sigma_v\approx\sigma_H\approx10^{-4}$ $Scm^{-1}$, regardless of oxygen partial pressure. At this temperature, pure protonic conductivity was not expected even at a high water vapor pressure, contrary to the previous works on $SrZrO_3$.[21,22] Same argument[8,23] was reported for $CeO_2$-based perovskites: Pure proton conduction was claimed from the measurements of the transference number in concentration cells. However, later workers provided evidences for both protonic and oxygen ion conduction; they carried out electrochemical pumping of oxygen and hydrogen using dry oxygen and dry hydrogen, respectively.[8,23] And they could explain the controversies associated with the transference numbers measured from a concentration cell technique. The likely reason is in the simultaneous establishment of $O_2$ or $H_2O$ concentration cell in the hydrogen concentration cell, and the effect of such secondary concentration cell was not properly taken into account. For oxygen or water concentration cells, similar problem is expected. Open circuit voltage in $H_2$ gas containing atmosphere can be given as one of the following expressions.[6,24]

$$V=-\frac{RT}{F}\int_{P_{H_2}'}^{P_{H_2}''}\frac{t_H}{2}d\ln P_{H_2}+\frac{RT}{F}\int_{P_{O_2}'}^{P_{O_2}''}\frac{t_v}{4}d\ln P_{O_2} \quad (26)$$

$$V=-\frac{RT}{F}\int_{P_{w'}}^{P_{w''}}\frac{t_v}{2}d\ln P_w-\frac{RT}{F}\int_{P_{H_2}'}^{P_{H_2}''}\frac{t_H+t_v}{4}d\ln P_{H_2} \quad (27)$$

$t_H$ and $t_V$ denote the respective transference number of

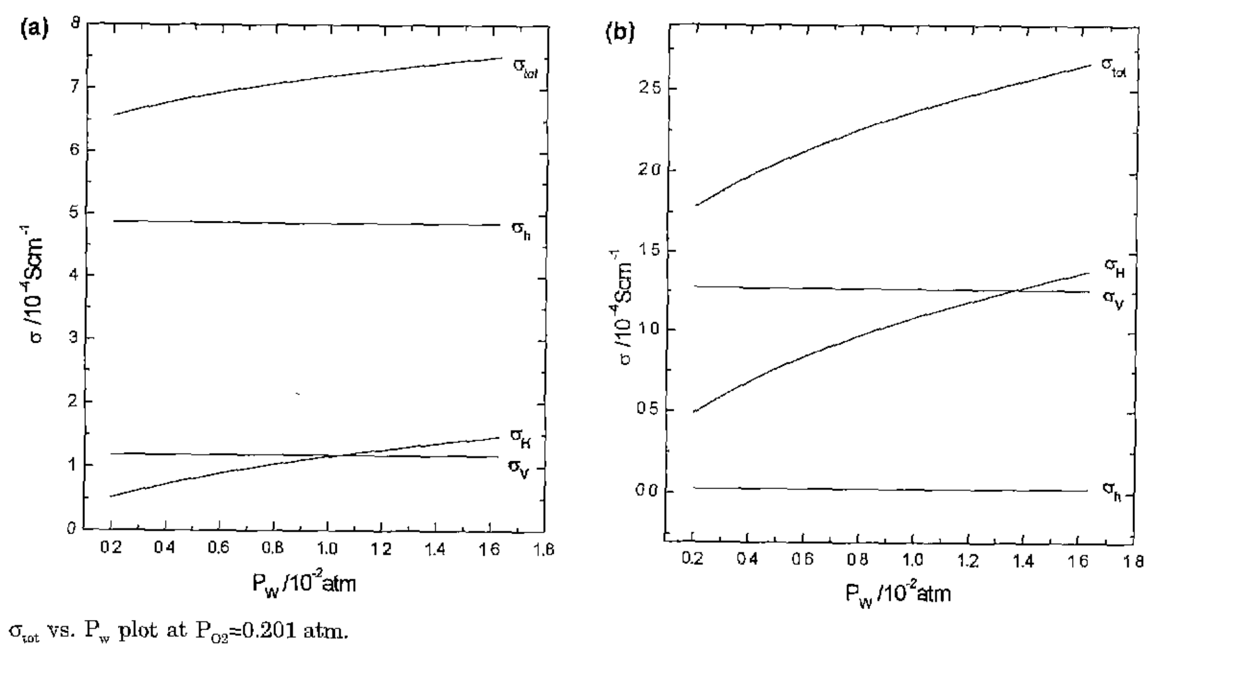


**Fig. 9.** (a) $\sigma_{tot}$ vs. $P_w$ plot at $P_{O2}$=0.201 atm.

proton and oxygen ion. R, T and F have their usual meaning. P' and P'' denote the partial pressures at the two electrodes. If Eq. (26) is chosen as a relevant expression, the open circuit voltage is a function by $P_{O2}$, in addition to $P_{H2}$. If composition of oxygen is not controlled and clearly specified, the results may be misleading.[25] For example, the transference number, if determined from a hydrogen concentration cell without consideration of $P_{O2}$ or $P_W$, may represent $t_H$ or $t_H+t_V$, depending whether the electrode condition is close to $P_{O2}'= P_{O2}''$ or $P_W'=P_W''$, respectively. (Fortunately the partial conductivities and thus transference numbers are not function of $P_{H2}$.[26])

To circumvent the limitations or requirements of stringent control of gas composition, $\sigma_{tot}$ vs. $P_{O2}^{1/4}$ technique has been preferred in the determination of ionic transference number.[7,8] Likewise, for the separation of proton and oxygen ion transference number, $_{tot}$ vs. $P_W^{1/2}$ technique is proposed in this work. The zirconate perovskites have similar characteristics of electrical properties; increasing conductivity with water vapor pressure,[15,17,27] and thus very low proton concentration and lower proton conductivities compared with cerate HTPCs.[23,28] At low enough oxygen partial pressures, the hole conductivity is suppressed and oxygen ion conductivity is almost constant against water vapor pressure, as mentioned earlier. Hence, the total conductivity is given as,

$$\sigma_{tot} \approx \sigma_v + \sigma_H \approx \sigma_v^* + \sigma_H^* P_w^{1/2} \qquad (28)$$

Obviously $\sigma_{tot}$ vs. $P_w^{1/2}$ plot enables to separate proton conductivity from total ionic conductivity.

## V. Conclusion

1. Total conductivity showed a linear increase in $\sigma_{tot}$ vs. $P_w^{1/2}$ plot for $SrZr_{0.95}Y_{0.05}O_{2.975}$ ceramics at 800°C. This is contrary to other HTPCs such as $SrCeO_3$ or $BaThO_3$-based perovskites, which exhibited a linear fall. The observed positive slope stems from the large α. The positive slope was also caused by relatively high $\sigma_H^*$ value, compared with $s_v^*$ or $\sigma_h^*$ of the material at the given temperature.

2. The parameter was determined to be in the range of $\alpha \geq 10$. The high α value represents the characteristic low proton concentration of zirconate HTPCs. α could become even higher due to a low activity coefficient of oxygen ion vacancies, in addition to the low equilibrium constant for the water dissolution reaction of the material.

3. The prediction of total conductivity showed a reasonable agreement with the experimental measurements. The calculation of partial conductivities at 800°C resulted in an almost pure ionic conductivity, contributed by both protons and oxygen ions, at $P_{O2}=10^{-10}$ atm and a predominant hole conductivity at $P_{O2}=0.20$ atm. The material is inherently p-type and oxygen ionic mixed conductor, and additional proton conduction was observed in wet atmosphere. No pure proton conductivity was expected even at low $P_{O2}$ and high $P_W$.

4. Oxygen ion conductivity is a very weak function of water vapor pressure in zirconate HTPCs, due to the low proton solubility. From the measurement of total conductivity versus $P_w$, it was shown that proton and oxygen ion transference number could be separated from total ionic conductivity at low oxygen partial pressures.

## Acknowledgment

This work was supported by the 1998 Hong-ik University Academic Research Fund.

## References

1. A. S. Nowick and Yang Du, "High-temperature Proton Conductors with Perovskite-related Structures," *Solid State Ionics*, **77**, 137-146 (1995).
2. N. Bonanos, "Transport Properties and Conduction Mechanism in High-temperature Protonic Conductors," *Solid State Ionics*, **53-56**, 967-974 (1992).
3. Y. Larring and T. Norby, "The equilibrium between Water Vapor, Protons, and Oxygen Vacancies in Rare earth Oxides," *Solid State Ionics*, **97**, 523-528 (1997).
4. H. D. Baek, "Modeling of Electrical Conductivity from $\sigma_{tot}$ vs. $P_{O2}^{1/4}$ Plot in wet Atmosphere for High-temperature proton-Conducting Oxides," *Kor. J. Ceram.* **4**(2), 136-140 (1998).
5. H. D. Baek, "Modeling of Electrical Conductivity in High-temperature Proton-conducting Oxides," *Solid State Ionics*, **110**, 255-262 (1998).
6. J. R. Frade, "Theoretical Behavior of Concentration Cells Based on $ABO_3$ Perovskite Materials with Protonic and Oxygen ion conduction,"*Solid State Ionics* **78**, 87-97 (1995).
7. E. K. Chang, A. Mehta, and D.M. Smyth, "Ionic Transport Numbers from Equilibrium Conductivities"; pp. 35-45 in proc. Symposium on Electro-ceramics and Solid-state Ionics, ed. by H. L. Tuller and D. M. Smyth, The Electrochemical Society, Inc., Pennington, 1988.
8. N. Bonanos, B. Ellis, K. S. Knight and M.N. Mahmood, "Ionic Conductivity of Gadollinium-doped Barium Cerate Perovskites," *Solid State Ionics*, **35**, 179-188 (1989).
9. Y. S. Chun, Master's Thesis, "Synthesis of proton conducting $SrZr_{0.95}Y_{0.05}O_{2.975}$ Powder by Citrate Gel Method," Hong-ik Univ., p. 47 (1997).
10. K. D. Kreuer, "On the Development of Proton Conducting Materials for Technological Applications," *Solid State Ionics*, **97**, 1-15 (1997)
11. F. Krug, T. Schober and T. Springer, "In Situ Measurements of the Water Uptake in Yb doped $SrCeO_3$," *Solid State Ionics* **81**, 111-118 (1995).
12. T. Tsuji and T. Suzuki, "Electrical Conduction in $BaThO_3$ with $Nd_2O_3$," *Solid State Ionics* **70/71**, 291-295 (1994).
13. T Tsuji, N. Miyajima, and M. Ochida, "Electrical conduction in $BaThO_3$ with $Y_2O_3$," *Solid State Ionics* **79**, 183-187 (1995).
14. H. Uchida, N. Maeda and H. Iwahara, "Relation between Proton and hole Conduction in $SrCeO_3$-based Electrolytes under Water-containing Atmosphere at high Temper-

atures," *Solid State Ionics*, **11**, 117-124 (1983).

15. N. Kurita, N. Fukatsu, K. Ito, and T. Ohashi,"Protonic conduction Domain of Indium-doped Calcium Zirconate," *J. Electrochem. Soc.*, **142**(5), 1552- 1559 (1995).
16. Y. Larring and T. Norby, "The Equilibrium between Water Vapour, Protons, and Oxygen Vacancies in Rare earth Oxides," *Solid State Ionics*, **97**, 523-528 (1997).
17. J. Müller, K. D. Kreuer, J. Maier, S. Matsuo, and M. Ishigame,"A Conductivity and Thermal Gravimetric Analysis of a Y-doped $SrZrO_3$ Single Crystal," *Solid State Ionics*, **97**, 421-427 (1997).
18. R. A. Swalin, Thermodynamics of solids, pp. 351-382, Wiley- interscience Publication, 2nd Ed., 1972.
19. K. D. Kreuer, Th. Dippel, Yu.M. Baikov, and J. Maier, "Water solubility, Proton and Oxygen Diffusion in Acceptor Doped $BaCeO_3$: A Single Crystal Analysis," *Solid State Ionics*, **86-88**, 613-620 (1996).
20. J. A. Labrincha, J. R. Frade and F. M. B. Marques, "Defect Structure of $SrZrO_3$," *Solid State Ionics*, **91**, 71-75 (1993).
21. T. Yajima , H. Suzuki, T. Yogo, and H. Iwahara, "Protonic Conduction in $SrZrO_3$-based Oxides," *Solid State Ionics*, **51**, 101-107 (1992).
22. H. Iwahara, T. Yazima, T. Hibino, K. Ozaki, and H. Suzuki, "Protonic Conduction in Calcium, Strontium and Barium Zirconates," *Solid State Ionics*, **91**, 65-69 (1993).
23. N. Bonanos, B. Ellis, and M. N. Mahmood, "Oxide Ion Conduction in Ytterbium-doped Strontium Cerate," *Solid State Ionics*, 28-30 (1988).
24. H. D. Baek, Unpublished work.
25. J. Guan, S. E. Dorris, U. Balachandran, and M. Liu, " Transport Properties of $BaCe_{0.95}Y_{0.05}O_3$. Mixed Conductors for Hydrogen Separation," *Solid State Ionics*, **100**, 45-52 (1997).
26. I. Kosacki, J. G. M. Becht, R. van Landschoot, and J. Schoonman, "Electrical Properties of $SrCe_{0.95}Yb_{0.05}O_3$ in Hydrogen Atmospheres," *Solid State Ionics*, **59**, 287-296 (1993).
27. T. Yazima, H. Kazeoka, T. Yogo, and H. Iwahara, "Proton Conduction in Sintered Oxides Based on $CaZrO_3$," *Solid State Ionics*, **47**, 271-275 (1991).
28. R. C. T. Slade, S. D. Flint, and N. Singh, "Investigation of Proton Conduction in Yb- and Y-doped Barium Zirconates," *Solid State Ionics*, **82**, 135-141 (1995).